III CONGRESO GEOLOGICO CHILENO
8-14 NOVIEMBRE 1982 CONCEPCION - CHILE

SAIRECABUR VOLCANO, a Plio-Quaternary calc-alkaline massif of the Andes of Atacama : Petrology.

DERUELLE Bernard

Department of Earth Sciences - Faculty of Science
University of Yaounde. B.P. 812, YAOUNDE (Cameroon).

ABSTRACT

Sairecabur volcano (Andes of Atacama) is a large Plio-Quaternary massif collapsed into a caldera. Sairecabur and Northern small cones erected after the collapse.

The lavas are andesites (pre-caldera lavas) and acidic andesites and dacites (post-caldera lavas) of the calc-alkaline association.

They contain phenocrysts of plagioclase, pyroxenes, magnetite (pre-caldera lavas) and hornblende, biotite and occasional quartz (post-caldera lavas). Crystal clots (pyroxene + plagioclase + magnetite) which result from the resorption of early crystallized hornblende phenocrysts are found. Crystallization of plagioclase phenocrysts took place under H_2O pressure of 1-4 kb and temperature of 850-950°C.

Major and trace element distributions indicate a differentiation of pre-caldera lavas by pyroxene + plagioclase fractionation and of post-caldera lavas by clinopyroxene + hornblende + plagioclase fractionation.

A three-stage model of petrogenesis is proposed : partial melting of peridotitic upper mantle, crustal contamination of the primitive magma at the base of the continental crust where crystal fractionation can begin and proceed during the more or less long ascent of the lava up to the surface.

INTRODUCTION

Sairecabur volcano is located on the border of the Altiplano of Atacama (Fig. 1). It consists in a large massif collapsed into a caldera. The massif is probably of Pliocene to Quaternary age as the oldest lavas are particularly unaltered and as their fresh aspect is similar to those of other volcanoes in adjacent areas which have Plio-Quaternary radiochronological ages (Roobol et al., 1976; Baker, 1977; Baker and Francis, 1978;

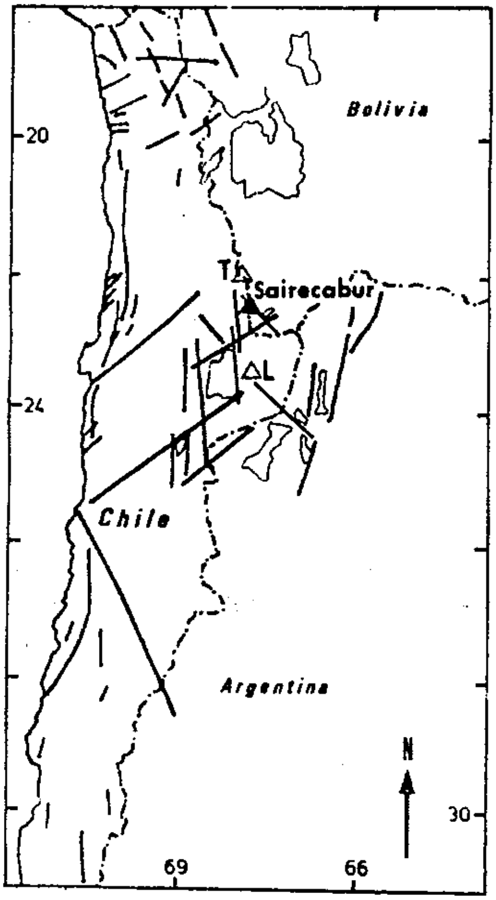

Fig. 1. Geographical location of Sairecabur volcano on the border of the Bolivian-Chilean Altiplano. Large faults are represented (after Chotin et al., 1978, modified). T and L: Tocorpuri and Lascar Plio-Quaternary volcanic massifs respectively.

Lahsen and Munizaga, 1979; Ramirez, 1979).

The volcano is located on large faulting zones oriented N135E and N65E (Déruelle et al., 1978) which give a rectangular shape to the contiguous Laguna Verde depression whereas N-S faults correspond to the direction of the hydrothermal alteration and characterize the Atacama graben (Fig. 2).

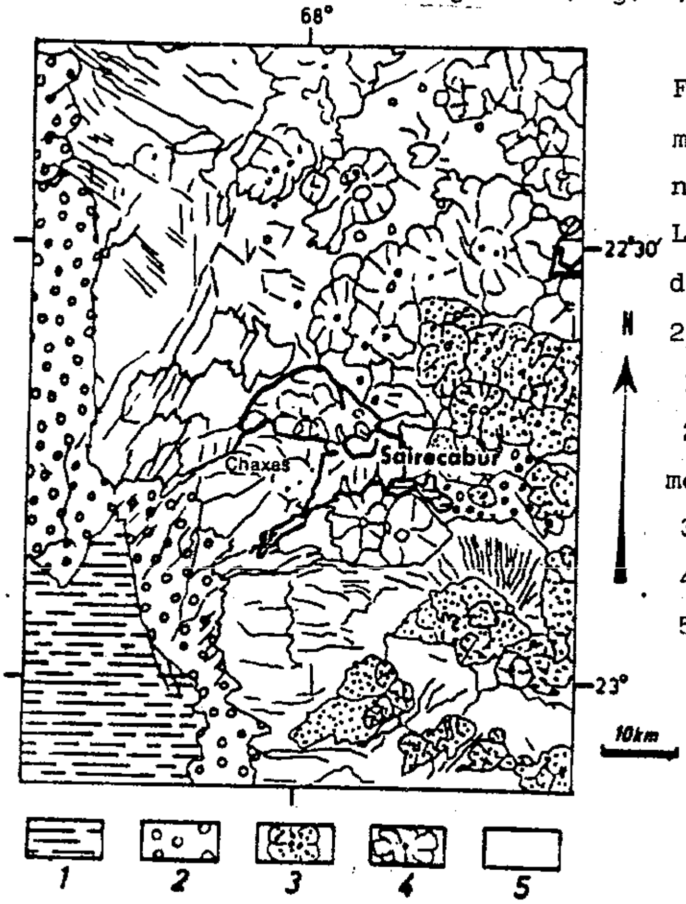

Fig. 2. Geological sketch map of the Sairecabur volcanic massif area obtained from LANDSAT imagery (NASA-ERTS document E-1243-14004, F.C.C. 23/April/1973).

1 : Salar of Atacama.

2 : recent and scree sediments.

3 : Pliocene volcanic cones.

4 : Plio-Quaternary cones.

5 : ignimbrites.

GEOMORPHOLOGY

The primitive volcano collapsed into a caldera of about 5 km diameter (Fig 3 a and b). The caldera is limited by a vertical cliff 400 m high. In the north, the cliff is covered with recent lava flows of the Sairecabur cone which is built upright the collapse fissure. Three secant craters cape this cone. An ultimate flow has been parted in two equivalent lobes, one of which reached the bottom of the caldera while the other one flowed down the northern flank of the primitive strato-volcano. Another cone, made of blcck lava flows has recently built up at the base of the northern flank of the primitive volcano. The flows of this northern cone

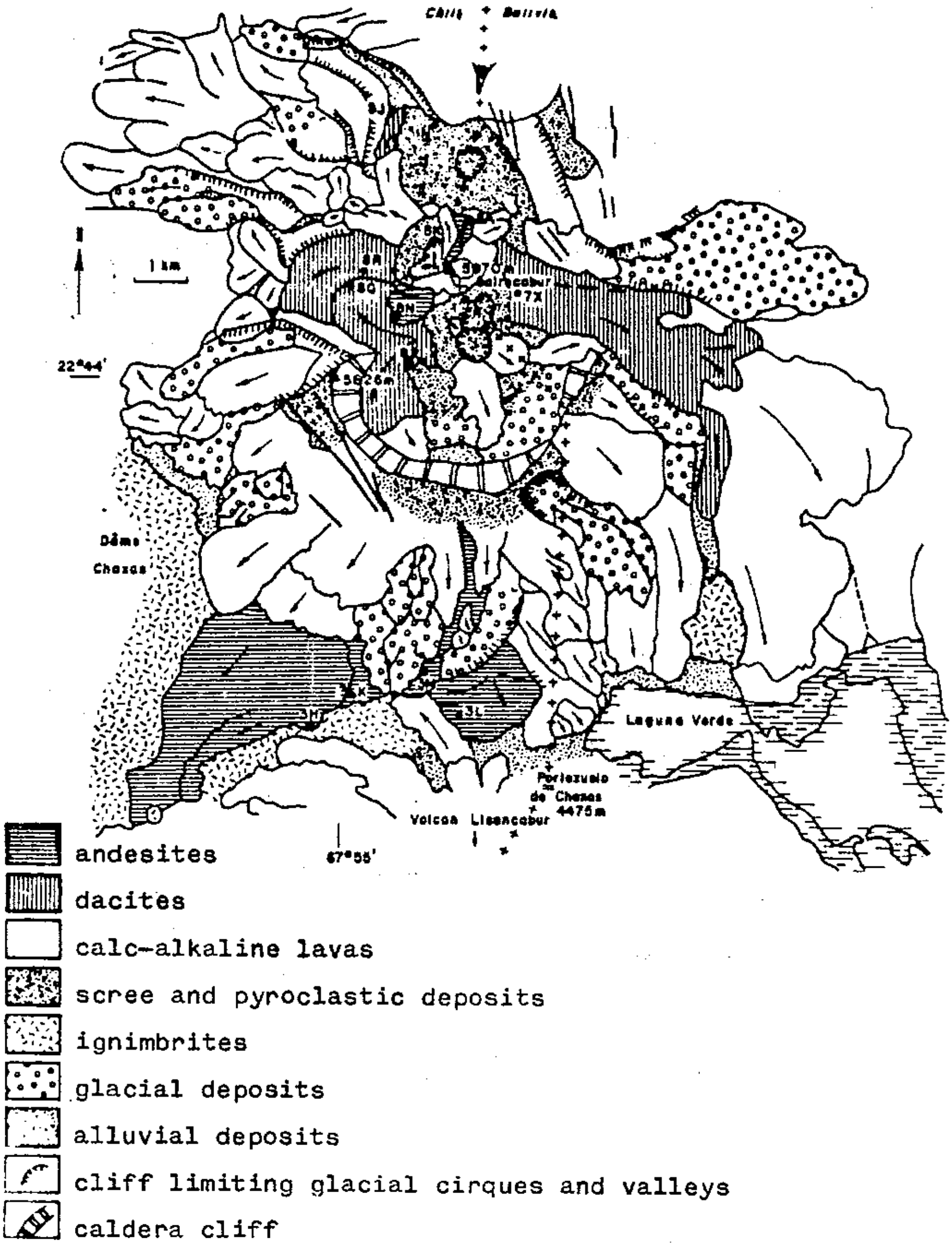

Fig. 3a. Geological map of Sairecabur massif. Geographical data, altitudes, scale and frontier drawing (crosses) are approximate. Sample numbers should be preceded by letter N. The map was drawn with use of aerial photographs n° 31-2662 to 2667, line 15A and 31-2622 to 2626, I.G.M., Santiago, and of western part of Sairecabur 1/50 000 topographic map, author spec. use, I.G.M. Santiago, unpublished.

Fig. 3 b. Aerial photograph of the western part of Sairecabur volcanic massif. Recent faults and cliffs are outlined. The summits are snow-capped. (After photograph n° 31-2664, line 15-A, 27-Apr-61, I.G.M., Santiago) are short and thick (some 10 m) as they are more acidic than those of the primitive strato-volcano which reach 20 km in length.

The strato-volcano has been deeply notched by glacial tongues.

N45E and N135E faults affect the southern flank of the primitive strato-volcano and cut recent flows which go around southern Licancabur volcano. Slickensides have sometimes swerved the course of posterior lava flows. Frontal moraines (ogives) cover the ultimate flows of Sairecabur cone.

If one builds up again the primitive strato-volcano towards its destroyed summit (Fig. 3 c), it appears that the summit could have reached an altitude of about 7 000 m; so the primitive volcano was one of the highest in the Andean Range (Ojos del Salado volcano is the uppermost with 6 885 m alt.) and in the world.

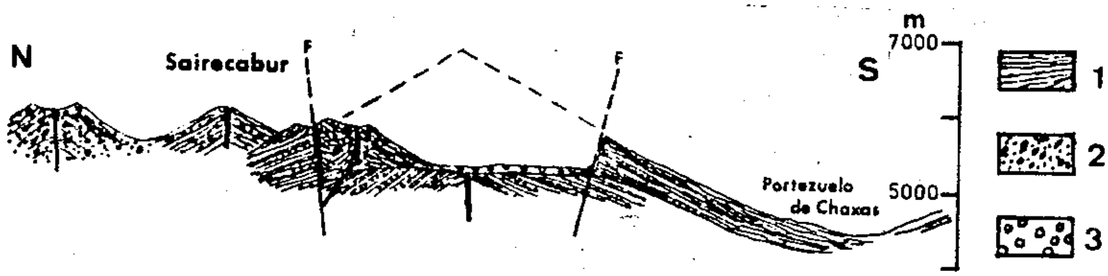

Fig. 3 c. Geological section across the Sairecabur massif.
1 : lava flows; 2 : pyroclastic deposits; 3 : glacial deposits.
F : faults limiting the caldera. The pipes are indicated with black lines. The primitive volcanic massive has been drawn according to its probable shape before collapse (light dashed line).

The presence of the contiguous ignimbritic massif of Chaxas, southwest of Sairecabur volcano (Fig. 2) should be related to the collapse of the caldera. The ignimbritic flows (7 M Years old, Ramirez, 1979) are dacites (Guest, 1969) and they have mostly spread towards the south-western graben occupied by the Salar of Atacama (2 500 m altitude). West of Sairecabur is located a little recent volcano (Puritama) whose lava flows (16 km long) follow the "quebradas" of faulting tectonic origin.

All the lavas studied in the present work have been attributed to the pre-caldera or post-caldera groups (see Fig. 3 a).

PETROGRAPHY

Pre-caldera lavas

The lavas are black and their texture is microlitic porphyric with more or less abundant glass. They often present a fluidal aspect. The distribution of the minerals is similar to those of pyroxene andesites of Atacama (Déruelle, 1979a). Plagioclase (An60-70), clinopyroxene, orthopyroxene and magnetite phenocrysts are found within a microlitic groundmass of plagioclase, clinopyroxene orthopyroxene and magnetite microlites and glass. N7X sample is altered by hydrothermal fumeroles and contains sulphur.

Post-caldera lavas

The lavas are black, greyish or brown and have desertic patine. They are characterized by hornblende phenocrysts. The phenocrysts are rather more abondant than in the pre-caldera lavas. Plagioclase (An40-60) is often cloudy. Orthopyroxene frequently includes clinopyroxene. Hornblende phenocrysts are destabilized and rimmed by opaque minerals or replaced by plagioclase, orthopyroxene, clinopyroxene and magnetite clots. Olivine has been found in one dacite (a common feature of dacitic lavas of Atacama) and is completely rimmed with orthopyroxene and plagioclase (An50). The mineralogical distribution corresponds to andesites (plg, cpx, opx, occasional hb) and dacites (presence of biotite) and this classification is in fair agreement with the chemical one.

MINERALOGY

Minerals have been studied under microprobe. The analyses are given in Table 1.

	Plagioclase					Cpx	Opx	Hornblende			Biotita		Mt	Ilm
	N3M	N3M	N3M	N8K	N8K	N3M	N3M	N8K	N8K	N8K	N8K	N8K	N3M	N3M
	Pc	Pb	m	Pc	Pb	P	P	P	mP	m	Pc	Pb	m	m
SiO_2	48.25	49.59	55.05	56.09	53.73	50.85	52.18	45.25	45.80	46.00	36.33	36.58	-	-
TiO_2	-	-	-	-	-	0.91	0.32	1.53	1.49	1.46	5.02	4.78	10.83	41.75
Al_2O_3	31.41	31.17	28.19	27.90	29.18	3.34	2.37	8.14	7.78	7.69	13.61	13.87	1.23	0.25
Fe_2O_3	-	-	-	-	-	-	-	-	-	-	-	-	39.32	9.90
FeO	0.90	0.79	0.36	-	-	8.20	14.81	13.99	13.84	14.15	16.09	15.43	42.17	37.75
MnO	-	-	-	-	-	0.36	0.53	0.38	0.35	0.40	0.10	0.20	-	-
MgO						16.37	29.10	14.07	14.41	14.35	14.64	14.71	-	-
CaO	15.91	15.40	10.94	8.85	9.63	20.40	1.48	11.55	10.73	11.30			-	-
Na_2O	2.28	2.49	4.70	6.07	5.36	0.50	0.26	1.40	1.31	1.47	0.67	0.68	-	-
K_2O	0.14	0.18	0.45	0.48	0.41			0.61	0.59	0.58	8.97	8.85	-	-
Total	98.91	99.62	99.69	99.62	98.50	100.92	100.03	97.01	96.33	97.43	95.42	95.14	93.55	89.70
Si	2.24	2.28	2.49	2.53	2.46	1.87	1.87	7.03	7.13	7.10	5.48	5.51	33.92 (1)	10.61 (2)
Ti						0.03	0.01	0.18	0.17	0.17	0.57	0.54		
Al	1.71	1.68	1.50	1.48	1.57	0.15	0.10	1.49	1.43	1.40	2.42	2.46		
Fe	0.03	0.03	0.01			0.25	0.44	1.81	1.80	1.82	2.03	1.94		
Mn						0.01	0.02	0.05	0.05	0.05	0.01	0.03		
Mg						0.90	1.52	3.26	3.36	3.33	3.27	3.30		
Ca	0.79	0.76	0.53	0.43	0.47	0.80	0.06	1.92	1.79	1.87				
Na	0.20	0.22	0.41	0.53	0.48	0.04	0.02	0.42	0.40	0.44	0.20	0.20		
K	0.01	0.01	0.03	0.03	0.02			0.12	0.12	0.11	1.73	1.70		
H_2O											3.97	3.98		

Table 1. Representative chemical analyses of the minerals of Sairecabur lavas CAMECA MS46 and CAMEBAX microprobe analysers in Lab. Petrography Univ. Paris VI and Lab. Petrography & Volcanology Univ. Paris XI, Orsay respectively. For plagioclase, pyroxenes, hornblende, biotite, magnetite and ilmenite : number of ions on the basis of 8, 6, 23, 22+2(OH), 32 and 6 oxygens respectively. P : phenocryst; m : microlite; c : core; b : border; mP : microphenocryst. 1: ulvospinelle, 2: hematite.

Plagioclase composition permits to evaluate (Kudo and Weill, 1970) the H_2O pressure of the plagioclase equilibrium, the temperature being deduced from microlitic Ti-Fe oxides equilibrium. Plagioclase phenocrysts equilibrated between 1 and 4 kb H_2O pressure. Crystallization temperature of pre-caldera andesite is 90°C higher than that of post-caldera dacite. Oxygen fugacities of pre-caldera andesites are just above the Ni-NiO buffer (Déruelle, 1979a) in the T-log f_{O_2} diagram of Buddington and Lindsley (1964).

Clinopyroxene is typical calcic augite with low Al^{VI}/Al^{IV}. Orthopyroxene is bronzite type and rather poorer in iron than Opx in orogenic zones. Opx-Cpx equilibration give temperatures around 950°C in pre-caldera andesites.

Hornblende is brown pargasitic hornblende which appears in phenocrysts, microphenocrysts and microlites. An attempt of replacement of hornblende has been made for the mineral phases which are observed in the clots (Table 2). The results differ from those of Steward (1975), but most of the clots in Sairecabur lavas still have the amphibole phenocrysts shape (Fig. 4) and are poorer in iron.

	Hb	Plg	Cpx	Opx	Mt	Qz
SiO_2	46.6	44.9	52.7	50.4	0.2	99.9
TiO_2	1.3	0.0	0.9	0.5	8.2	0.0
Al_2O_3	8.2	31.8	3.0	2.7	2.0	0.1
FeO	13.9	0.1	6.4	15.2	81.0	0.0
MnO	0.4	0.0	0.6	0.6	0.6	0.0
MgO	13.6	0.3	16.4	28.2	0.6	0.0
CaO	11.7	16.4	20.4	1.2	0.0	0.0
Na_2O	1.3	5.1	0.4	0.3	0.1	0.0
K_2O	0.3	0.1	0.1	0.1	0.0	0.0
%	100.0	19.4	40.2	24.6	9.3	4.4
St Dev.		3.5	10.6	2.3	9.9	9.2

Table 2. The chemical composition of hornblende coincids with the global chemical composition of the clots according to the modal distribution of the minerals. Calculations have been made without quartz here introduced in replacement of glass; the results are quite the same (after Wright and Doherthy (1970) calculations method).

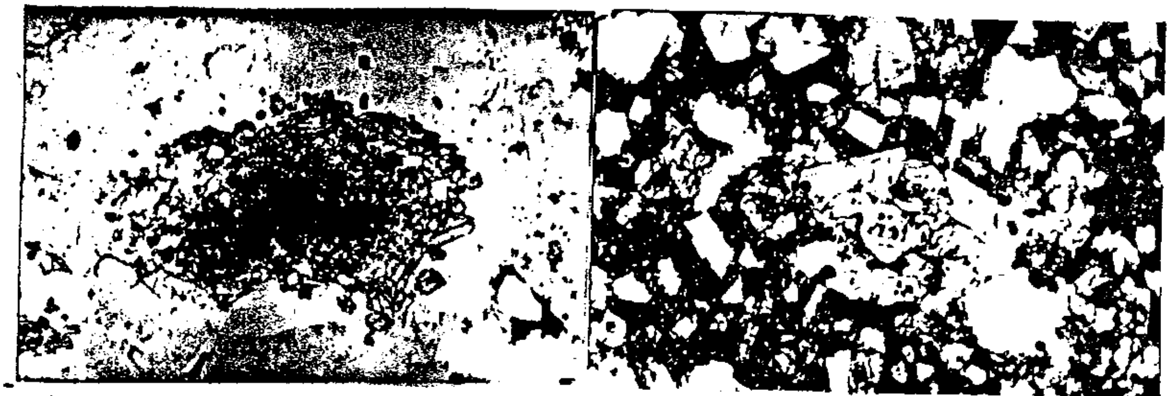

Fig. 4. Hornblende phenocrysts on the way to breakdown as hypersthene + plagioclase + augite + magnetite clots. |———| : 1 mm.

Biotite phenocrysts are often broken or folded. They crystallize in the ultimate stages of the magmatic differentiation and they are not altered. It is difficult to distinguish biotite from hornblende microlites but under microprobe test. Biotite is rich in TiO_2 (as observed in Peruvian dacites, Andriambololona, 1976).

Quartz phenocrysts are scarce in two dacites. They are highly corroded and distinct from those found in shoshonitic lavas from Argentina (Déruelle, 1979a) as these latter are rimmed by microlitic pyroxenes.

Iron oxides are abundant in phenocrysts compared to andesitic lavas from other volcanoes of Atacama. Ilmenite is rare and generally not ubiquitous. Oxides contain few MnO, even in differentiated lavas.

Zircon and apatite are found as accessory minerals.

GEOCHEMISTRY

AFM diagram (Fig. 5) gives a good distinction between the two pre- and post-caldera groups of lavas (Table 3).

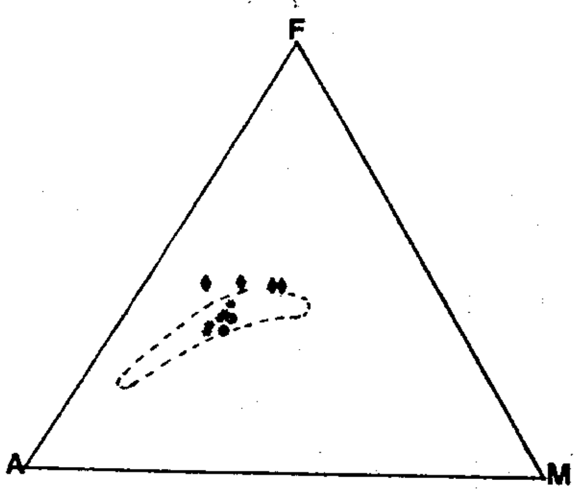

Fig. 5. AFM diagram ($F = FeO + 0.9\ Fe_2O_3$). ♦ : pre-caldera lavas; ✱ and ● : respectively Northern and Sairecabur cones of the post-caldera lavas group. The dashed line limits distribution fields of andesites and dacites from Tocorpuri (Déruelle, 1979b) and Lascar (Déruelle, 1979a) neighbouring volcanoes (see Fig. 1).

In the MgO – FeO diagram (Fig. 6), the pre-caldera lavas trend shows light iron enrichment with differentiation. If pyroxene fractionation may explain the pre-caldera lavas trend, differentiation of post caldera is probably dominated by hornblende (and/or biotite) fractionation. As observed in the calc-alkaline lavas of Atacama (Déruelle, 1979a) thorium is a good differentiation index. The

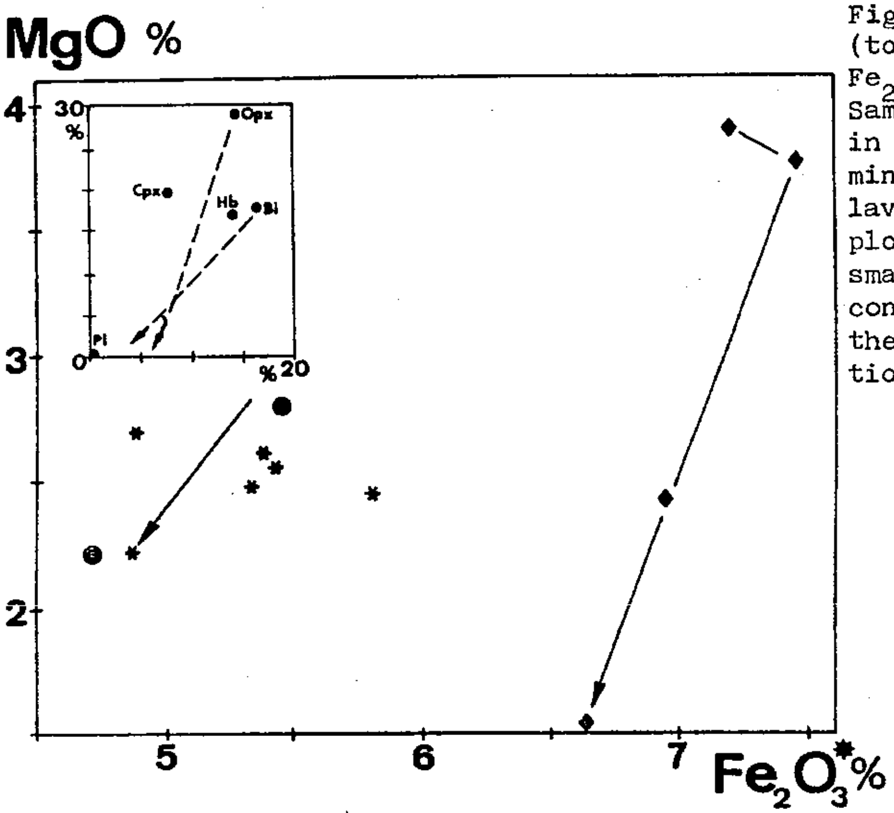

Fig. 6. MgO - Fet (total iron as Fe_2O_3) diagram. Same symbols as in Fig. 5. The minerals of the lavas have been plotted in the small diagram conjointly with the differentiation trends.

Fig. 7 offers a good discrimination between the three groups of lavas : 1 : precaldera, 2 : Sairecabur cone and 3 : Northern cone.

Major elements.

Pre-caldera and Sairecabur cone lavas show a correlative decrease in MgO, CaO and increase in SiO_2, TiO_2, Na_2O and K_2O with differentiation which correspond to pyroxene fractionation. Variations in iron distribution could arise from changes in the relative proportions of orthopyroxene and clinopyroxene.

Post-caldera lavas (Northern cone) show smooth decrease in CaO, Fe_2O_3, TiO_2 and Na_2O while MgO remains rather constant with increasing differentiation as a result of clinopyroxene fractionation followed by hornblende and plagioclase fractionations.

Trace elements.

Sr and Rb show a good correlation (Fig. 8). Sr decrease with

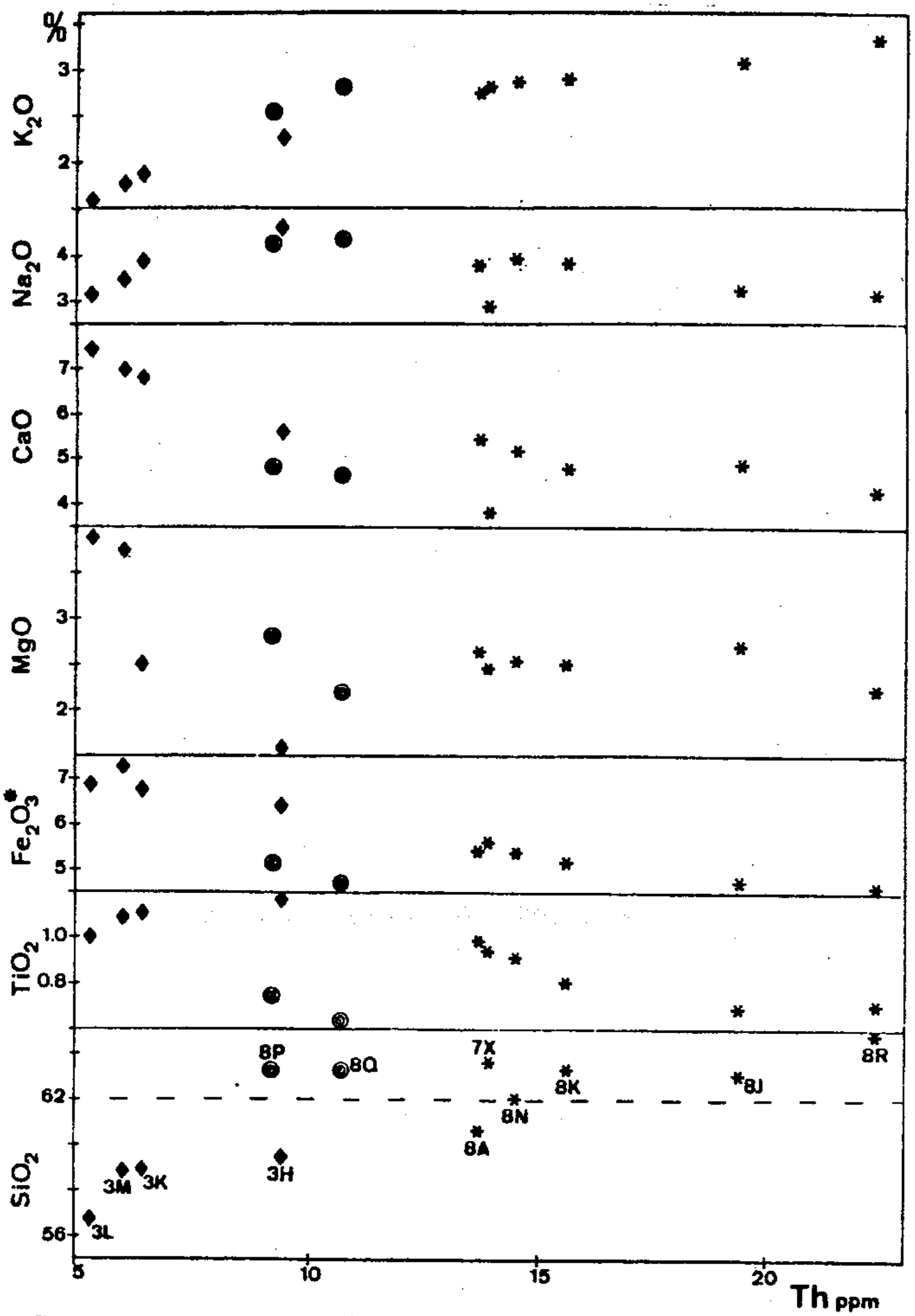

Fig. 7. Major elements vs Th diagram. Same symbols as in Fig. 5. The lavas are classified in andesites (SiO_2 < 62%) and dacites (SiO_2 > 62%).

	N3L	N3M	N3K	N3I	N8A	N8N	N8J	N8P	N7X	N8Q	N8F	N8R
SiO_2	56.67	58.76	58.87	59.41	60.60	61.99	63.01	63.24	63.27	63.31	63.32	64.86
TiO_2	1.01	1.09	1.11	1.18	0.98	0.92	0.69	0.74	0.94	0.64	0.80	0.71
Al_2O_3	17.66	16.93	17.46	17.30	16.70	16.46	15.82	16.30	13.26	16.66	15.94	15.07
Fe_2O_3	3.20	1.92	2.02	2.18	5.37	5.42	4.87	1.60	5.80	4.71	1.71	1.57
FeO	3.56	4.95	4.39	3.98				3.44			3.23	2.95
MnO	0.11	0.12	0.08	0.10	0.07	0.07	0.07	0.10	0.07	0.08	0.09	0.08
MgO	3.88	3.76	2.44	1.53	2.62	2.56	2.69	2.79	2.44	2.21	2.48	2.21
CaO	7.47	7.01	6.79	5.64	5.38	5.14	4.88	4.85	3.85	4.62	4.75	4.26
Na_2O	3.08	3.25	3.44	3.80	3.37	3.45	3.13	3.61	2.91	3.66	3.38	3.04
K_2O	1.57	1.77	1.88	2.27	2.76	2.88	3.08	2.56	2.83	2.81	2.90	3.31
P_2O_5	0.25	0.31	0.19	0.28				0.25			0.27	0.18
H_2O+	1.15		0.18	0.97	0.86	0.14	1.16	0.46	3.80	0.40	0.31	1.52
H_2O-	0.29	0.09	0.13	0.22				0.22			0.16	0.28
Li	12	10	12	19	25	25		21	20	25	27	33
Rb	46	55	55	67	96	104	126	88	99	96	114	145
Sr	468	465	477	416	482	453	350	422	459	447	411	307
Ba	422	460	487	598	603	613	521	565	573	624	581	510
Cs	1.4	1.6	1.4	1.9	4.6	4.9	8.0	3.3	4.7	4.0	5.3	8.7
V	189	231	224	197	155	148	135	146	136	126	160	133
Cu	23	21	22	19	10	10	10	10	10	10	10	10
Cr	78	85	40	29	54	50	74	61	69	42	56	50
Co	21	21	17	13	13	14	12	12	11	10	13	10
Ni	23	21	10	0	11	13	16	13	8	7	12	8
Sc	20	20	18	17	13	13	13	12	12	11	13	12
Sb	0.1	0.1	0.1	0.2	0.6	0.6	1.0	0.3	1.0	0.4	0.6	1.1
Zr	153	170	187	211	198	174	137	194	150	196	198	144
Hf	4.2	4.7	4.9	6.1	5.6	5.1	4.2	4.5	4.6	4.9	5.0	4.8
Ta	0.65	0.73	0.78	1.06	1.05	1.12	1.37	0.89	1.06	1.03	1.13	1.46
La	21.6	22.9	24.3	32.6	35.3	35.2	32.2	27.8	27.9	31.2	35.0	37.5
Ce	61	65	60	98				75			87	
Sm	4.3						4.6					4.9
Eu	1.29	1.32	1.46	1.71	1.34	1.26	1.09	1.15	0.86	1.13	1.26	1.06
Tb	0.55	0.62	0.65	0.84	0.52	0.52	0.51	0.52	0.36	0.53	0.51	0.52
Yb	1.65						1.46					1.56
Lu	0.29						0.25					0.27
Th	5.3	6.0	6.4	9.4	13.7	14.5	19.4	9.2	13.9	10.7	15.6	22.4
U	1.4	1.7	1.8	2.5	4.0	4.0	6.2	2.8	4.0	3.4	4.4	6.8

Table 3. Chemical analyses of lavas from Sairecabur volcanic massif. Major elements in wet %; traces in ppm. Major elements, V and Cu : automated optical emission spectrochemical analyses (Govindaraju et al., 1976); Li, Rb, Sr, Ba : atomic absorption spectrophotometry (Dupuy and Lefèvre, 1974); other elements : neutronic activation analyses (Chayla et al., 1973). Isotope work at Oxford by S. Moorbath, mass spectrometer analyses (Pankhurst and O'Nions, 1973): $^{87}Sr/^{86}Sr$ = 0.70801 and 0.70845 for samples N3H and N8A respectively.

differentiation corresponds to pyroxene fractionation in pre-caldera lavas while lower Sr contents correlated with higher Rb contents in the other lavas correspond to plagioclase and hornblende fractionations. Ba is concentrated in biotite which fractionates only in the ultimate stages of the differentiation (Fig. 9) simultaneously with hornblende. The same results are deduced from Cs distribution.

There is a strong decrease in transition elements with increa-

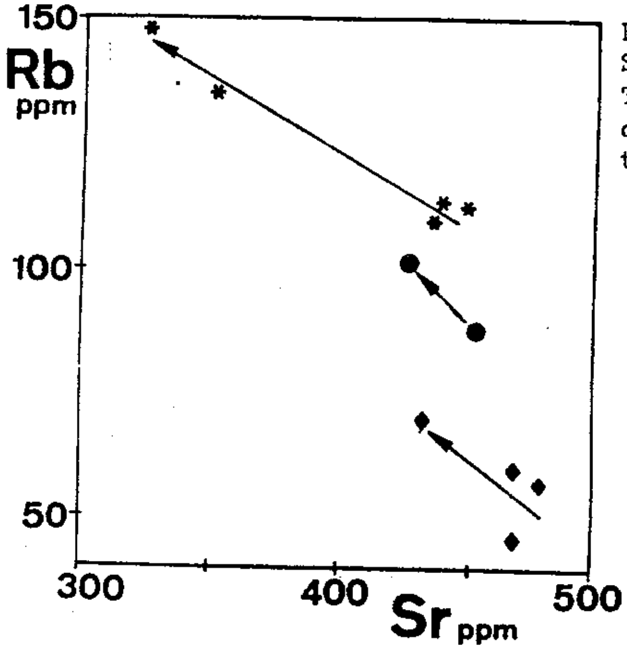

Fig. 8. Sr - Rb diagram. Same symbols as in Fig. 5. The arrows indicate the increasing differentiation of the lavas.

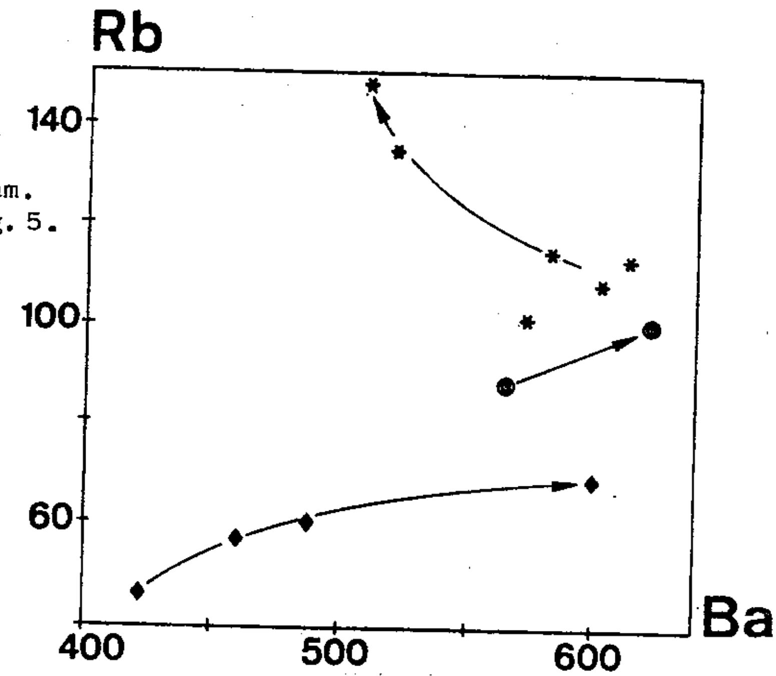

Fig. 9. Rb - Ba diagram. Same symbols as in Fig. 5. Arrows : see Fig. 8.

sing differentiation particularly in pre-caldera lavas. Two distinct trends (Joron et al., 1978) appear for post-caldera lavas in the Ni - Th diagram (Fig. 10). Crystal fractionation of magma bubbles issued from partial melting of a basic primitive magma is clea-

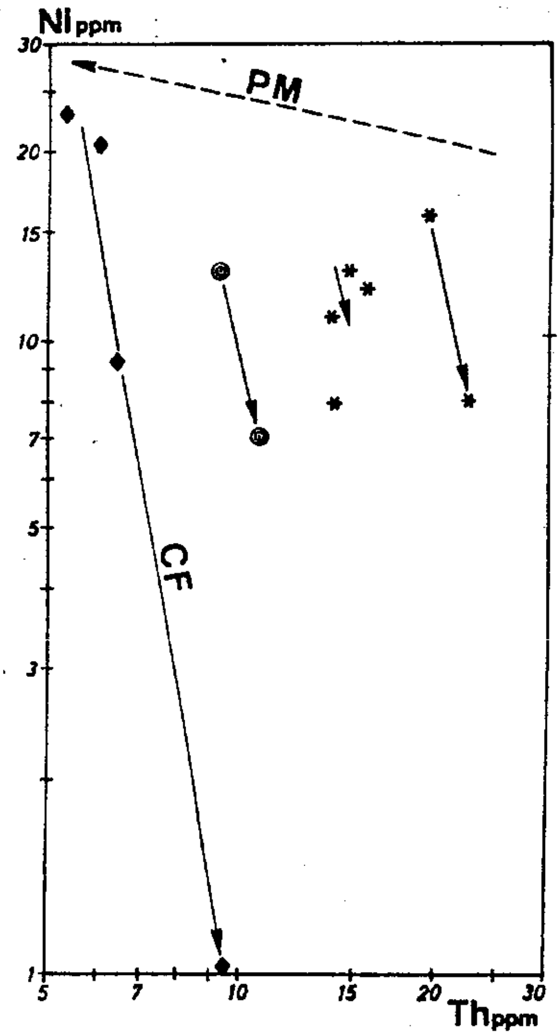

Fig. 10. Ni – Th diagram. Same symbols as in Fig. 5. The progress of partial melting (PM, dashed line) of a primitive magma and of crystal fractionation (CF, full lines) of individual magma bubbles are indicated by the arrows.

ly put on evidence. The trends of differentiation of the lavas correspond to various stages of crystal fractionation of a material resulting from various stages of partial melting of a common source. Same results are obtained with Co, Cr, Sc distributions. Cu contents are remarkably low in post-caldera lavas compared with those of post-caldera lavas.

Hf and Zr have reverse trends in pre and post-caldera lavas (Fig. 11). Biotite fractionation is probably effective in the latest differentiated lavas of post-caldera stage. Th and Ta or Tb give another example of crystal fractionation of magmas derived from var-

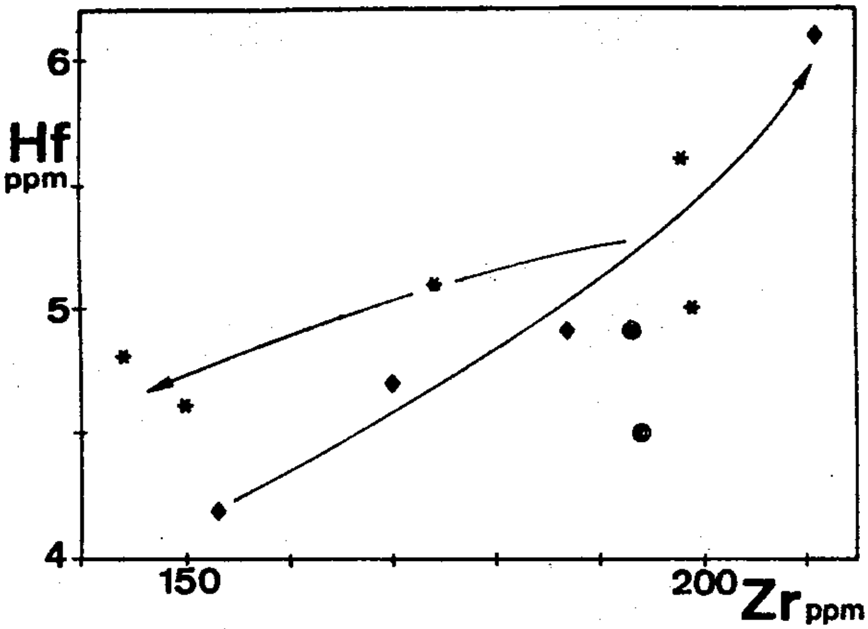

Fig. 11. Hf - Zr diagram. Same symbols as in Fig. 5. The differentiation trends are indicated with arrows.

ious degrees of partial melting of a basic source (Fig. 12).

Heavy rare earth elements fractionate more intensively than light rare earth elements as a result from hornblende precipitation in acidic lavas. No europium depletion is observed as no potassic feldpar interferes in the differentiation of the lavas.

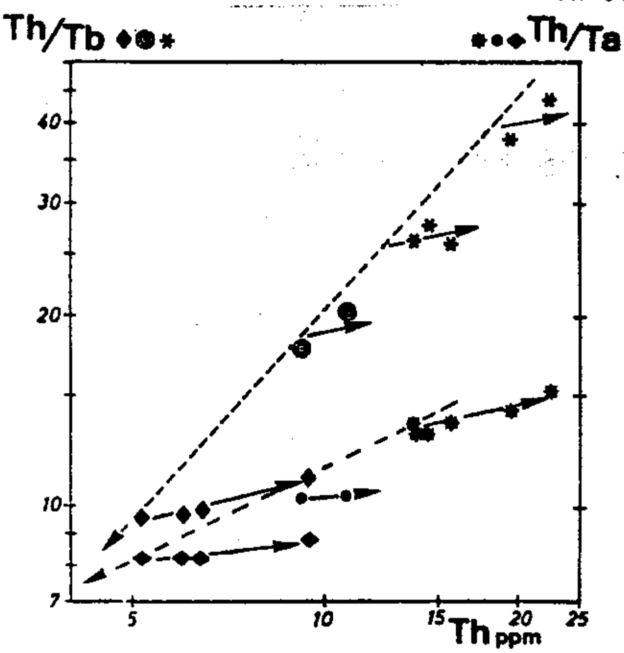

Fig. 12. Th - Th/Tb and Th/Ta diagram. Same symbols as in Fig. 5. The dashed and full lines correspond respectively to partial melting of a magmatic source and to crystal fractionation. The arrows indicate the progress of these processus (as explained in Joron et al., 1978).

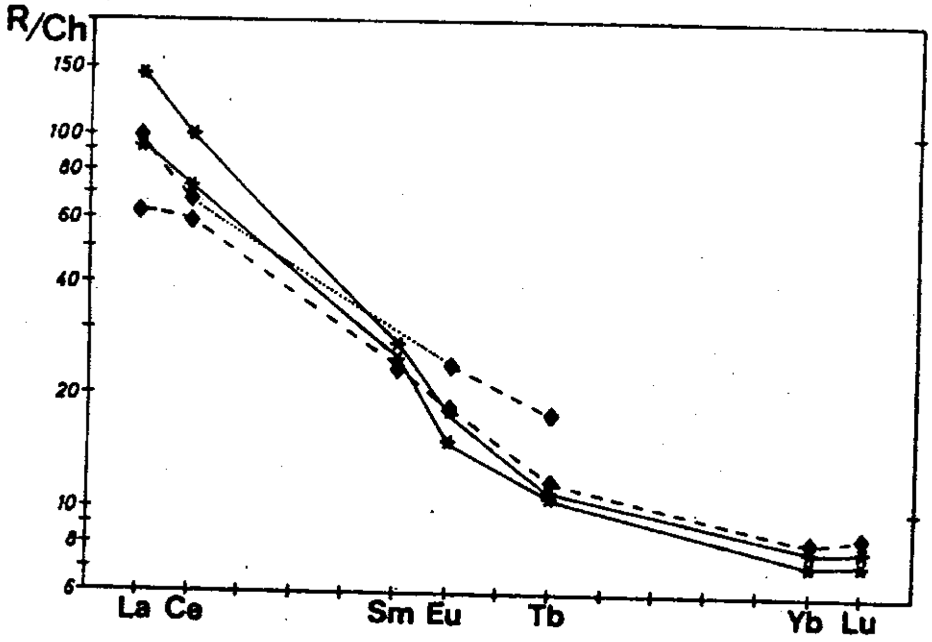

Fig. 13. Chondrites normalized REE patterns. Same symbols as in Fig.5. Pre and post-caldera distribution fields are limited by dashed (and dotted) and full lines respectively. Chondrites data after Frey et al., 1968.

Sr isotopic ratios do not show great variation between pre- and post-caldera lavas. No contamination of the magmatic source can be detected between the two episodes of the volcano erection. The original material is the same for the two lava series.

PETROGENESIS

Partial melting of peridotitic upper mantle can lead to andesites by means of ol + plg + cpx + mt fractionations. Major elements modelling is consistent with such hypotheses (Lopez-Escobar et al., 1977; Déruelle, 1979a). If REE distribution can be explained by the occurrence of garnet in peridotites, Sr isotopic ratios and K, Rb, Ba, Sr concentrations are not satisfactory with the upper mantle origin. As a generally admitted fact, single stage models of the genesis of calc-alkaline magma are inconsistent with the previously exposed data. Common limitations to single stage process arise from the absence of xenoliths in the lavas, large-ion-lithophile element distribution and Sr isotopic data. The model proposed hereafter is not far from numerous ones that have been elaborated since Taylor's

(1969) contribution. It inserts into the Andean geophysical and geological frames critically reviewed in Déruelle (1979a).

The first stage of the magma genesis is supposed to occur in the peridotitic upper mantle of the American plate, when fluids escape from the Nazca descending lithospheric slab and induce melting of the overlying peridotitic upper mantle. Bubbles of primary magma are generated. The degree of melting does not need to be higher than 15% (Déruelle,1979a). Variations in degrees of melting of the upper mantle and in the rate of contamination give the magmatic identity of the volcano unity. Crystal fractionation can begin at great depths (pressure $>$ 20 kb) and proceed up to the base of the continental crust. Amphibole clots correspond to deep crystallization of basic magma.

The main effect of the second stage is contamination of the primary magma by continental material at the base of the lower continental crust. The rate of contamination depends on the more or less long duration of the stay (from years to M. y.) of the primary magma at the base of lower crust where LILE or incompatible elements are concentrated. In this zone "an extensive basement reactivation and a melting may be expected" (Moorbath, 1978).

Crystal fractionation predominates during the third stage. Simultaneous occurrences of phenocrysts of olivine, plagioclase, clinopyroxene, orthopyroxene, hornblende and biotite in the same lava is the proof of a continuous process of equilibrium-disequilibrium of the different mineral phases during variations of the thermodynamic conditions. Distributions of phenocrysts reflects the evolution of the fractional crystallization with increasing differentiation. Hornblende and biotite are more dependent on temperature of crystallization than on water pressure which always complies with crystallization conditions of hydrated phases. High oxygen fugacity favours oxide fractionation but not in such a determining way as exposed by Osborn (1979). Crystal fractionation processes are shortened when the ascent of the lava is fast; basic lavas of South-Central Andes (such as pre-caldera lavas of Sairecabur) were emitted along large fractures which facilitate their ascent. Post-caldera lavas result from late emissions of residues of a primitive bubble of magma which stayed a long time in the continental crust after the collapse of the caldera which obturated the feeding lava chimneys; they are characterized by low pressure ($<$20 kb) "continental" crystal fractionation.

CONCLUSIONS

The lavas from Sairecabur massif are representative of volcanic activity in active continental margins. The petrography, the mineralogy and the geochemistry of the lavas can be explained by a three-stage model of genesis : partial melting of peridotitic upper mantle, crustal contamination of the primitive magma at the base of the continental crust and crystal fractionation during the more or less long ascent of the lava up to the surface.

ACKNOWLEDGEMENTS

Field work was carried out in Chile during stay at the Northern University, Antofagasta (1974-75; Dir. Prof. S. Espinoza) under the auspices of the French-Chilean Scientific and Technical Cooperation. Major and trace element analyses have been realized thanks to the financial support of R.C.P. 339 (Dir. Prof. J. Aubouin, Pierre et Marie Curie Univ., Paris). The author is grateful to J.-L. Joron for neutronic activation analyses (Pierre Süe Lab. Res., Saclay (France), Dir. Prof. M. Treuil) and to Dr S. Moorbath (Dept Geol. Mineral., Univ. Oxford, Great-Britain) for Sr isotopic measurements. H. Bizouard (Dept Petrogr. Volcanol., Univ. Paris XI, Orsay, France) and M.-C. Magonthier (Dept. Petrol., Univ. Pierre et Marie Curie, Paris) are acknowledged for their assistance in microprobe analyses.

REFERENCES

ANDRIAMBOLONA, R. D., 1976. Les éléments de transition dans les suites andésites et shoshonitiques du sud du Pérou. These, Univ. Sci. Tech. Languedoc, Montpellier (France), 88 pp.

BAKER, M. C. W., 1977. Geochronology of Upper Tertiary volcanic acticity in the Andes of North Chile. Geol. Rundsch., 66, 455 - 467.

BAKER, M. C. W. and FRANCIS, P. W., 1978. Upper Cenozoic volcanism in the Central Andes, ages and volumes. Earth Planet. Sci. Lett., 41, 175 - 187.

BUDDINGTON, A. F. and LINDSEY, D. H., 1964. Iron-titanium oxides minerals and synthetic equivalents. J. Petrol., 5, 310 - 357.

CHAYLA, B., JAFFREZIC, H. and JORON, J.-L., 1973. Analyse par activation dans les neutrons épithermiques. Application a la détermination d'éléments en traces dans les roches. C. R. Acad. Sci., Paris, 277, D, 273 - 275.

CHOTIN, P., DERUELLE, B. and GIRET, A., 1978. La marge Andine Argentino-Chilienne observée de l'espace (premieres données et perspectives). 6° Réun. An. Sci. Terre, Soc. Géol. Fr., 103.

DERUELLE, B., 1979a. Pétrologie d'un volcanisme de marge active: Atacama et Andes Méridionales. These Doct. Etat, Univ. Paris XI, Orsay, 418 pp.

DERUELLE, B., 1979b. Les volcans de Tocorpuri: pêtrologie des laves et genese magmatique. Seg. Congr. Geol. Chileno, Arica (Chile), Inst. Invest. Geol. Santiago E213-222.

DERUELLE, B. Petrology of the Plio-Quaternary volcanism of the South-Central and Meridional Andes. 26° Inter. Geol. Congr., Paris (1980), J. Volc. Geothermal Res., in press.

DERUELLE, B., CHOTIN, P. and GIRET, A., 1978. Une vision synoptique des liaisons volcano-structurales dans la marge active andine: l'exemple de la région d'Atacama (Chili, 21-25° S). Rev. Géogr. Phys. Géol. Dyn., 2, 20, 259-268.

DUPUY, C. and LEFEVRE, C., 1974. Fractionnement des éléments en trace Li, Rb, Ba, Sr dans les séries andésitiques et shoshonitiques du Pérou. Cimparaison avec d'autres zones orogéniques. Contrib. Mineral. Petrol., 46, 147-157.

FREY, F. A., HASKIN, M. A., POETZ, J. and HASKIN, L. A., 1968. Rare earth abundances in some basic rocks, J. Geophys. Res., 173, 6085-6098.

GOVINDARAJU, K., MEVELLE, G. and CHOUARD, C., 1976. Automated optical emission spectrochemical bulk analysis of silicate rocks with microwave plasma excitation. Anal. Chem., 48, 1325-1330.

GUEST, J. E., 1969. Upper Tertiary ignimbrites in the Andean Cordillera of part of the Antofagasta Province, Northern Chile. Geol. Soc. Am. Bull., 80, 337-362.

JORON, J.-L., BOUGAULT, H., WOOD, D. A. and TREUIL, M., 1978. Application de la géochemie des éléments en traces a l'étude des propriétés et des processus de genese de la croute océanique et du manteau supérieur. Bull. Soc. Géol. Fr., 7, 20, 521-531.

KUDO, A. M. and WEILL, D. F., 1970. An igneous plagioclase thermometer. Contrib. Mineral. Petrol., 25, 52-65.

LAHSEN, A. and MUNIZAGA, F., 1979. Nuevos antecedentes cronológicos del volcanismo cenozoico superior de los Andes del Norte de Chile entre los 19°30' y los 22°15' latitud Sur. Seg. Congr. Geol. Chileno, Arica (Chile), Inst. Invest. Geol., Santiago, F61-82.

LOPEZ-ESCOBER, L., FREY, F. A. and VERGARA, M., 1977. Andesites and high-Al basalts from Central-South Chile High Andes: geochemical evidence bearing on their petrogenesis. Contrib. Mineral. Petrol., 63, 199-228.

MOORBATH, S., 1978. Age and isotope evidence for the evolution of continental crust. Phil. Trans. Roy. Soc. London, A, 288, 401-413.

OSBORN, E. F., 1979. The reaction principle. Ir H.S. Yoder Jr (Editor), The evolution of the igneous rocks. Fiftieth anniversary perspectives. Princeton Univ. Press, Princeton, New-Jersey, U. S. A., 133-169.

PANKHURST, R. J. and O'NIONS, R. K., 1973. Determination of Rb/Sr and $^{87}Sr/^{86}Sr$ ratios in some standard rocks and evaluation of X-ray fluorescene spectrometry in Rb-Sr geochemistry. Chem. Geol., 12, 127-136.

RAMIREZ, C. F. R., 1979. Edades potasio-argon de rocas volcánicas cenozoicas en la zona de San Pedro de Atacama- El Tatio. Región de Antofagasta. Seg. Congr. Geol. Chileno, Arica (Chile), Inst. Invest. Geol., Santiago, F31-41.

ROOBOL, M. J., FRANCIS, P. W., RIDLEY, W. I., RHODES, M. and WALKER, G. F. L., 1976. Physico-chemical characters of the Andean volcanic chain between latitudes 21° and 22° South. Symp. Andean Antartic Volc. Prob., I. A. V. C. E. I., Spec., 450-464.

STEWARD, D. C., 1975. Crystal clots in calc-alkaline andesites as breakdown products of high-Al amphiboles. Contrib. Mineral. Petrol., 53, 195-204.

TAYLOR, S. R., 1969. Trace element chemistry of andesites and associated calc-alkaline rocks. St. Oregon, Dept. Geol. Min. Indus. Bull., 65, 43-63.

WRIGHT, T. L. and DOHERTY, P. C., 1970. A linear programming and last squares computer method for solving petrologic mixing problems. Geol. Soc. Amer. Bull., 81, 1995-2008.